Investigations on the Effect of Design Parameters on the Velocity Distribution in Swirling Fluidized Bed: An Experimental Study

Jessy Kochumman[1], Christopher Ezhil Singh Sreedharan[2], Vishal John Mathai[1], Mary Little Flower Thomas[3], Glan Devadhas George[4], Sridharan Ponnusamy, Jerril Gilda Sreedharan[5] and Jaya Christiyan Kumaravelu Grace JesyBai[6]

[1]Department of Mechanical Engineering, Amal Jyothi Engineering College, Kottayam, Kerala, India
[2]Department of Mechanical Engineering, Vimal Jyothi Engineering College, Kannur, Kerala, India
[3]Department of ECE, St. Xavier's Catholic College of Engineering, Kanyakumari, Tamil Nadu, India
[4]Director of Research and Innovation, CMR University, Bengaluru, Karnataka, India
[5]Department of EEE, Sri Muthukumaran Institute of Technology, Chennai, Tamil Nadu, India
[6]Department of Mechanical Engineering, Ramaiah Institute of Technology, Bangalore, Karnataka, India

Correspondence to:
K. Jessy,
kjessy@amaljyothi.ac.in

Additional material is published online only. To view please visit the journal online.

Cite this as: Jessy K, Singh SCE, Mathai VJ, Flower ML, Devadhas GG, Sridharan P, Gilda SJ and Christiyan KGJ. Investigations on the Effect of Design Parameters on the Velocity Distribution in Swirling Fluidized Bed: An Experimental Study. Premier Journal of Science 2025;15:100254

DOI: https://doi.org/10.70389/PJS.100254

ABSTRACT

Swirling fluidized bed machining (FBM) is a non-traditional method of abrasive machining which is a variant of FBM and finds its application in the polishing of surfaces with complex geometry with passages and grooves. Current research focus up on computational fluid dynamics (CFD) analysis by varying design parameters to identify their effect on velocity distribution and pressure drop across the air distributer. Various design parameters considered for CFD analysis using SOLID WORKS software are distributer hole diameter, distributer hole inclination, plenum chamber depth and air-inlet velocity. The simulation results in the form of charts, tables, graphs, images and animations emphasize that the optimized values of design parameters chosen for CFD have shown almost the same value of maximum velocity and same pattern in the velocity distribution across the cylindrical container. An experiment was also conducted to validate the optimized design parameters. Both the experimental as well as theoretical analysis results confirmed that maximum value of jet velocity with uniform pattern, encompass a region 10–170 mm from the distributer position across the cylindrical container. This region is identified as the region of maximum abrasive – metal interaction during SFM, which will result in fastest and effective surface modification.

Keywords: Swirling fluidized bed machining, CFD velocity distribution, Distributor hole inclination, Plenum chamber depth optimization, Abrasive surface finishing

Introduction

In Swirling fluidized bed machining (SFBM), the compressed air empowered by a centrifugal blower emerges out through a porous distributer with inclined holes (150) with the plane containing the plate. The air emerging out of the inclined holes possess jet velocity which has three components at any point in any plane within the cylindrical container (Figures 1 and 2). Radial component is responsible mixing of air, tangential component empowers swirling of the air and the axial component supports fluidization within the cylindrical container. The combined effect of these three components defines swirling fluidized bed (SFB) activity. Now if abrasive grains of various grades of silicon carbide / Alumina are made to accumulate over the distributer plate, they will be forced to attain the transportational properties of air and will vigorously agitate within the cylindrical column in a swirling fluidized state. The fluidized air and particle mixture now can be accessible to any grooves and passages of any component with complex geometry. Any metallic specimen with poor surface finish if placed property within the container and subjected to SFBM, the abrasive particles will impinge on the surface and cause metal removal and surface finish. The velocity of abrasive particles and air mixture can be controlled by adjusting the air flow rate. Main components of an SFBM setup as in Figure 2 are (a) Centrifugal blower which supplies compressed air (b) A pipe connecting to plenum chamber facilitating tangential entry of the air to plenum chamber (c) Distributer plate, which is the most vital component with inclined holes, facilitating swirling and fluidized motion (d) Plenum chamber, a cylindrical column fitted below the distributer in which the air column builds up a steady swirling pattern to facilitate smooth entry in to the inclined distributer holes (e) Cylindrical container fitted above the distributer through which the air emerges out of the inclined holes and swirl with fluidized motion vigorously, powered by three components of velocity in tangential, axial and radial directions. The distributer is fastened between the upper flange and lower flange attached to cylindrical and plenum chamber respectively (f) A work piece holder, which is conveniently clamped within the cylinder so that the work piece can be fitted at the suitable angle and height and (g) A cone or cylinder which is provided at the centre of cylindrical container to prevent accumulation of abrasive grains at the centre due to the centrifugal action.

Barletta et al.[1] experimentally analysed the influence of various process variables on the effectiveness of fluidized bed machining (FBM). As part of their research, they identified the machining variables as machining time, air inlet velocity, abrasive grain size, material hardness, abrasive type and shape factor to analyse their effect on metal removal rate (MRR) and surface roughness. Srinivasan et al. and Jun et al.[2–4] experimentally analysed the hydrodynamic features of SFB. The experimental set up involved a centrifugal blower, plenum chamber distributer with inclined vanes at 120, and a cylindrical container. It was observed that the particles on the bottom layer move in circular path mainly confined to the bottom portion. They possess much more velocity and increased concentration when compared to fluidized bed (FB). The horizontal component of velocity (V cos α) supports swirling motion and vertical component (V sin α) facilitates the fluidization. They employed the design parameters such as plenum chamber (height 600 mm, dia 300 mm), tangential pipe (120 ϕ) distributer (300 mm diameter) with vane angle 120, and cylindrical container (300 mm diameter and height 600 mm) after the optimization experimentally.

Peer Review
Received: 16 August 2025
Last revised: 27 December 2025
Accepted: 27 December 2025
Version accepted: 6
Published: 31 January 2026

Ethical approval: N/a
Consent: N/a
Funding: N/a
Conflicts of interest: N/a
Author contribution:
Jessy Kochumman, Christopher Ezhil Singh Sreedharan, Vishal John Mathai, Mary Little Flower Thomas, Glan Devadhas George, Sridharan Ponnusamy, Jerril Gilda Sreedharan and Jaya Christiyan Kumaravelu Grace JesyBai – Conceptualization, Writing – original draft, review and editing
Guarantor: Jessy K
Provenance and peer-review: Unsolicited and externally peer-reviewed
Data availability statement: N/a

It was observed that in the case of SFB, a uniform fluidization can be achieved even with lower distributor pressure drop which is a distinct advantage of SFBs.

Paulose et al.[5] while studying the hydrodynamic behaviour of SFB with different type of distributers on the SFB setup, designed and developed inclined hole type of distributers by embedding copper tubes in araldite. It was observed that distributors with 150 inclined holes possess more useful area (94%) when compared to single row vane type distributer with 150 inclination (64%). The design parameters included were diameter (300 mm), inclination of hole to the horizontal (150 and 200), diameter of hole (3 mm), radial pitch (10 mm), thickness of distributer (10 mm), centre cone diameter (75 mm) and total number of holes (285 & 480).

Barletta et al.[6] observed the limitations of FBM in which the top portion of the work piece (specimen) is not able to machine effectively due to the screening effect. The surface closer to bottom portion of the cylinder is subjected to better surface modification. Faizal et al.[7] conducted CFD simulation studies on velocity distribution of air in a SFB by using distributer with 10°, 15°, 20° inclination and observed that the distributer with 45 blades and 150 inclination is the best considering the better flow unity and low pressure drop.

Francis et al.[8,9] developed SFBM as a novel variant of FBM using SFBM set up with the same design parameters but with the distributer with inclined holes. The investigations focused on analysis the effect of process parameters such as abrasive grain size, velocity of impact, machining time, materials properties etc. on machining performance in terms of MRR and surface finish. While investigating the effectiveness of SFBM process It was tested a straight spur gear for surface finishing and the results showed that a difference in roughness value (Ra) 1.5 μ between various locations could be brought down to 0.24 μ within 2 hours of processing.

Further conducted the research to study the role of various metal cutting mechanisms during the metal – abrasive interaction. It was observed through SEM and optical microscopy that micro – cutting mechanisms like ploughing, fatigue, cutting, sliding and rolling impact play significant roles in varying levels owing to the change in impact speed of abrasives and materials properties. An attempt to machine brass specimen with various grades of abrasive progressively (from 20, 40, 60, 80, 100 and 120) proved that Ra value from 1.3 μ could be brought down to 0.18 μ after 7 hours of processing. A comparative study further revealed that SFBM can perform better machining than FBM owing mainly to two reasons (a) Chain like movement of abrasive particles in the former case causing faster machining and (b) The drawback of screening effect is completely eliminated in SFBM. Jun et al.[4] observed that abrasives with high impact speed result in faster surface modification but prolonged machining tend to damage the surface in softer materials. Zhang et al.[10] shows that optimizing cyclone efficiency and reducing coal particle size in CFB boilers improves bed material quality and alters gas–solid flow, thereby reducing NOx emissions. Enhanced cyclone performance creates a reducing atmosphere and increases fine char particles, effectively inhibiting NOx formation. Adjustments in coal feeding and volatiles release patterns further enhance emissions control and combustion efficiency. Simanjuntak et al.[11] explores low-rank coal drying in a fluidized swirl bed with varying guide vane angles and temperatures. The smaller angles and higher temperature enhanced the drying rates and energy efficiency. The Khazaei and Rational models best described the drying kinetics with high accuracy (R^2 = 0.9980–0.9992). Zhang et al.[12] addresses heat and mass transfer limitations in micro-fluidized bed reactors for gas–solid endothermic reactions by using a 3D Eulerian model. Innovations such as a squid-fin-inspired wall and corrugated vortex generator improved fluid dynamics, heat transfer, and methane conversion by 26%. Such a new reactor design makes possible the determination of precise kinetic parameters for rapid, heat-intensive reactions. The paddy drying kinetics in the SFB dryer was investigated by Sitorus et al.[13] at different capacities of 1–3 kg, a temperature of 55°C, and a drying time of 45 minutes. The linear-plus-exponential model fitted the best to predict moisture content with a high R^2 of 0.9867 and RMSE of 0.0395. Drying capacity significantly affected the drying behavior; higher capacities influence the drying rate.

In the treatment of low concentration lead polluted groundwater, the researchers Ban et al.[14] in this study created a novel microporous flocculation magnetic fluidized (MFMFB) reactor that obtained a greater than 98% efficiency for the removal of Pb(II) and turbidity using optimum dosages of flocculant and optimized dynamics of flow within the reactor utilizing a magnetic levitation layer that increases the rate of mixing as well as the adsorption within the reactor. Some researchers have performed computational fluid dynamics (CFD) simulation of a fluidized bed system. Pietrobono et al.[15] investigated the statistical correlation of the sample position and uniformity on the aluminum substrate that was machined using FBM. They proved that the sample position on the bed cts surface morphology of the aluminum substrate during the process of FBM. In very recent times, there are reports on an application of FBM for the finishing of metal 3D printing products.[16]

Since microcutting acts as an ineffective mechanism in removing metal due to rolling having the mechanism of impact, the surface wear rate is optimized when the work piece is kept perpendicular to the abrasives' flow direction.[17]

Kim et al.[18] study combined experiments on stainless steel 304 (SS304) with alumina particles and CFD simulations to analyze process parameters. Results of the study indicated that the MRR increases with rotation speed peaking at 0.04 MPa air pressure and that CFD was useful in equipment design and optimization. The main aim of this research is to offer a new surface finishing method in the form of a nonconventional machining process. This new method has the potential to develop as an alternative surface finishing process that may significantly reduce the surface roughness on the components with the so-called complex passages and the surface finish is mainly a function of the grain size of the abrasives like Al_2O_3 and SiC.

Having established the feasibility and effectiveness of SFBM as a surface modification process, the first objective of this paper is to theoretically identify the maximum velocity regions during SFB activity to identify best suitable values of design parameters such as air inlet velocity, distributer hole inclinations, hole diameter, plenum chamber depth etc. to optimize the machining process. The second objective is to analyse their effect on distributer pressure drop and velocity distribution. Experimental verification of the CFD findings comes under the third objective. Both objectives were identified as gaps in the literatures.

Materials and Methods

CFD Modelling and Simulation

The first part deals with the CFD analysis of SFB design parameters for which the modelling of a SFB set up for SFB activity using SOLIDWORKS software. The modelling involves the designing of each component with the dimensions as in the experimental set up. Main individual components are Plenum chamber to which air enters tangentially (dia-300 mm and height-600 mm), Cylindrical container in which the fluidized air swirl (dia-300 mm and height-600 mm), tangential pipe connecting the blower with plenum chamber (dia-120 mm) and the distributer plate mounted between plenum chamber and the cylindrical container (thickness-10 mm and dia-300 mm). The design parameters such as hole diameter, hole inclination and plenum chamber depth were varied accordingly based on the boundary conditions of the respective CFD as listed in Table 1. The assembly was subjected to simulation. The results were analysed based on the generated images, graphs and animations.

The CFD analysis is planned to investigate the effect of air – inlet velocity (CFD-1), effect of distributor-hole inclination (CFD-2), effect of hole diameter CFD-3) and the effect of plenum chamber depth (CFD-4) on the nature of jet velocity distribution within the cylindrical container. In order to maximize the abrasive – metal interaction in SFBM, it is important to locate the region of highest velocity as well as concentrated flow pattern. Table 1 enlists the boundary conditions applied in each case of CFD.

The conclusions are drawn from the generated graphs, charts and simulation images. Since the pressure drop across the distributer plays a significant role in determining the velocity distribution and maximum jet velocity in the empty bed the pressure at a plane 10 mm above and below the distributer was recorded in order to estimate the pressure difference.

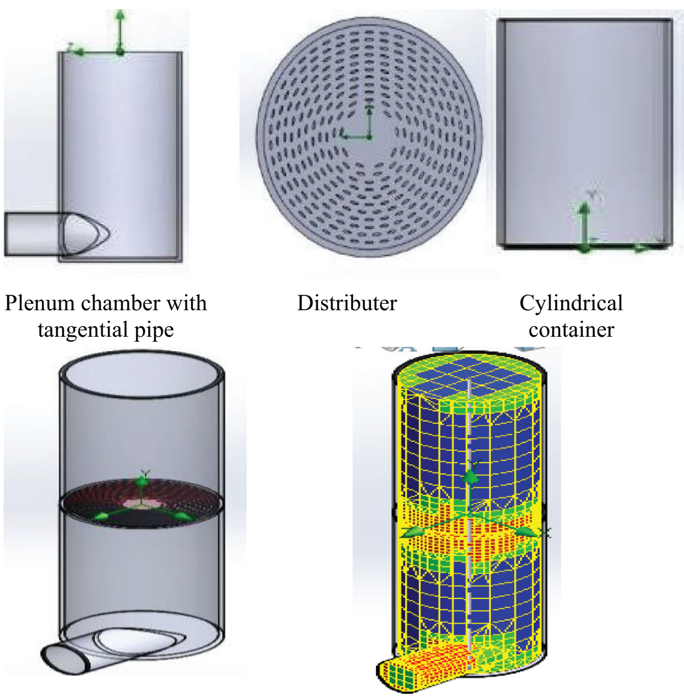

Fig 1 | SFB components in modelling stage

Experimental Evaluation

In order to experimentally verify the findings from CFD analysis, a work piece of aluminium was subjected to SFBM on the experiment setup powered by Centrifugal blower. The experiment was conducted under the operating conditions as shown in Table 2. The work piece surface was given an initial roughness of 1.4 μ by means of applying emery paper of grade 120 in order to generate a rough surface equivalent to a machined rough surface.

The work piece was clamped vertically with its bottom edge making a clearance of 35 mm. After half an hour processing the work piece was taken to

Table 1 | Effect of CFD design parameters on velocity distribution in the SFB container: boundary conditions

CFD Study		Fluidizing Media: Air; No. of Distributer Holes: 285			
Sl. No.	Design Parameter Details	Boundary Conditions			
		Air Inlet Velocity (m/s)	Distributer Hole Inclination (deg.)	Distributer Hole Dia. (mm)	Plenum Chamber Depth (mm)
1	Effect of air-inlet velocity	2, 3, 4, 6, 8	15	3	600
2	Effect of distributer hole inclination	4	13, 15, 17, 20	3	600
3	Effect of Distributer hole dia.	4	15	1, 2, 3, 4, 5, 6	600
4	Effect of plenum chamber depth	4	15	3	300, 400, 500, 600, 700, 800

Fig 2 | SFBM experiment set up

Table 2 | Operating conditions for SFBM experiment set up

Velocity of Air-Intake	4.11 m/s
Abrasive type	SiC Grit Size 20
Quantity of abrasive	500 g
Work piece material	Aluminium 5052 (30 mm × 100 mm)
Initial roughness	1.4 μm
Number of hours	30 minutes
Distributor	Inclined hole type (15°)

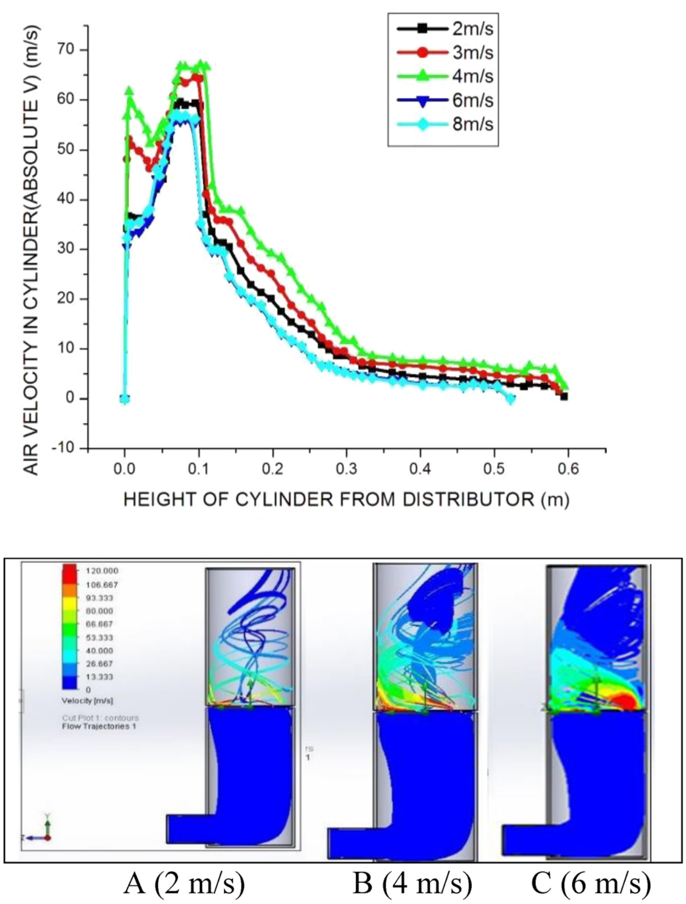

Fig 3 | Velocity distribution in cylinder at different heights varying air inlet velocity. (a) 2 m/s, (b) 4 m/s, (c) 6 m/s

Metallurgical lab for characterization. The work piece was cleaned well using acetone and subjected to microscopic analysis and the surface morphology was recorded at different points, length wise. The roughness was also tested at these points using profilometer and roughness value recorded in terms of R_a at Measurements lab.

Results and Discussion

For investigating the effect of air inlet velocity (m/s) on the velocity distribution within the cylindrical container, the boundary conditions were applied as in Table 1. The simulation results are demonstrated in the form of images and graphs as shown in Figure 3 which represents the velocity distribution in cylinder at different heights varying air inlet velocity. The total height of the cylinder is 600 mm as per the design. The characteristic curves in all cases (2, 3, 4, 6 and 8 m/s) show a uniform pattern and maximum velocity distribution lies at a height of 150 mm from the distributer level (considered as reference). It is evident from the graph that at air inlet velocity of 4 m/s, highest value of jet velocity of 65–70 m/s was observed within 0–150 mm limit. However, a little consideration will show that the high velocity region can be extended to 200 mm height, owing to the significant velocity distribution of 30–40 m/s in this region. The velocity curves at different inlet velocities then shows a linear down ward trend up to 300 mm (middle portion of the cylinder) and thereafter maintain velocity of 0–13 m/s in second half portion. This is mainly because of the gradual weakening of the three components of velocity (tangential, axial and radial) as the height increases.

Distributor pressure drop is an important parameter, which influences the energy consumption and the fluidization quality. In general, a higher distributor pressure drop leads to higher energy consumption.

Figure 4 represents change in pressure drop across the distributer varying SFB design parameters. During the first CFD analysis, the pressure drop across the distributer between bottom and top portions was characterized for different air-inlet velocities such as 2, 3, 4, 6, and 8 m/s. A gradual increase in pressure drop (Figure 4a), is visible as the velocity increases. As the velocity of flow increases, the frictional force also increases resulting in dip in the pressure head above the plane of the distributer which leads to rise in the jet velocity of emerging air from the inclined holes.

Although the highest value of jet velocity is in the range of 55–70 m/s as in the graph (Figure 3), it is interesting to note that the simulated images clearly explain the difference in the pattern of the flow of air (Figures 3a–c) respectively for 2, 4, and 6 m/s. In the case of velocity 4 m/s, the swirling fluidized air flow assumes uniform, concentrated and evenly pattern for the 1/3rd portion of the cylindrical container as compared to other two velocities (2 and 6 m/s). The air flow to the SFB set up is determined by the regulating mechanism using ventury meter or pitot tube.

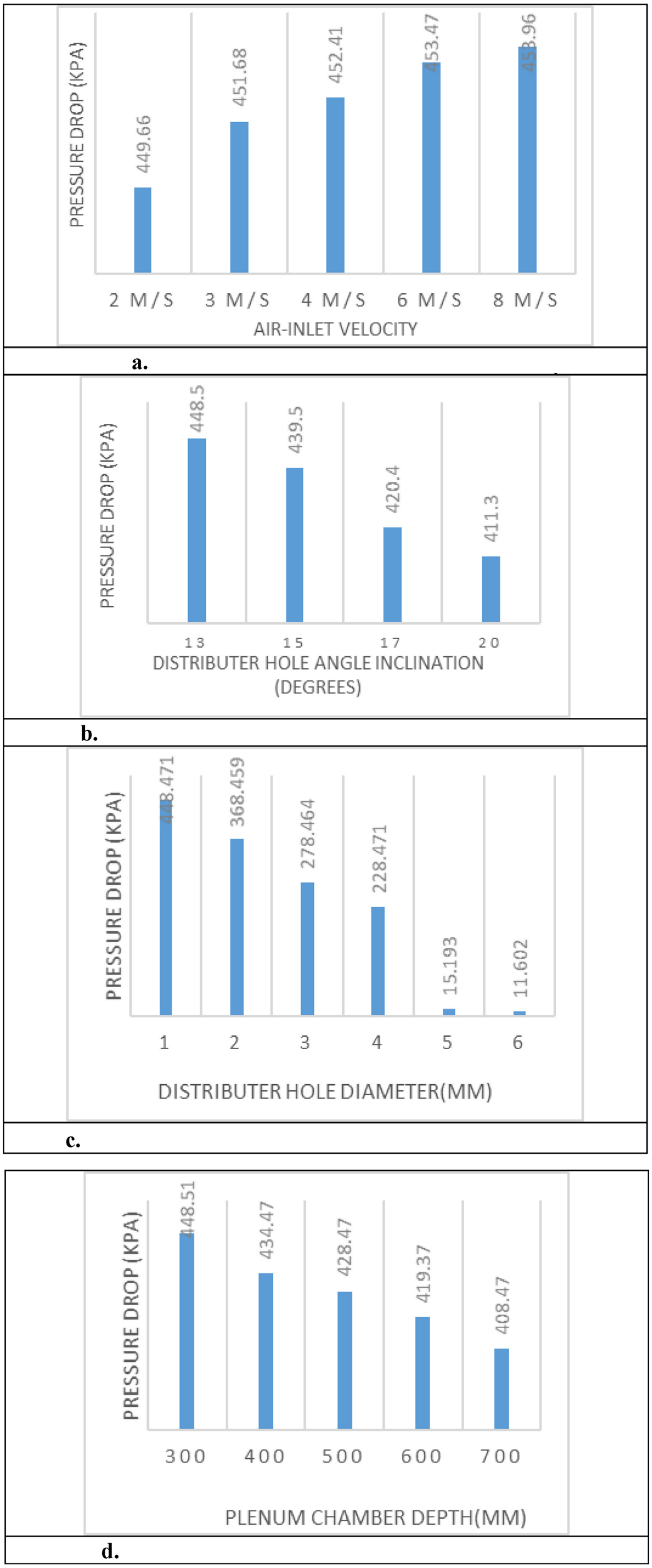

Fig 4 | Change in pressure drop across the distributer varying SFB design parameters. (a) Pressure drop varying Air-inlet velocity. (b) Pressure drop varying distributer hole inclination. (c) Pressure drop varying distributer hole diameter. (d) Pressure drop varying plenum chamber depth

The SFB experimental set up design is having a limited capacity which is capable of passing air at a velocity in the range of 4 m/s only. Distributor pressure drop is an important parameter, which influences the energy consumption and the fluidization quality. In general, a higher distributor pressure drop leads to higher energy consumption. Figure 4 represents change in pressure drop across the distributer varying SFB design parameters. During the first CFD analysis, the pressure drop across the distributer between bottom and top portions was characterized for different air-inlet velocities such as 2, 3, 4, 6, and 8 m/s.

A gradual increase in pressure drop (Figure 4a), is visible as the velocity increases. As the velocity of flow increases, the frictional force also increases resulting in dip in the pressure head above the plane of the distributer which leads to rise in the jet velocity of emerging air from the inclined holes.

During the second CFD analysis (Figure 4b), the pressure drop across the distributer between bottom and top portions was characterized for different distributer hole inclinations such as 13°, 15°, 17° and 20°. The pressure difference recorded shows rise, ranging from 411 KPa to 448 KPa as the hole inclination decreases. This can be attributed to the abrupt change in the flow direction at lower angles as the air from the plenum chamber enters the distributer. Another reason for the rise in the pressure drop is high frictional resistance offered by hole surface as the passages are longer at lower inclinations, resulting in high distributer pressure drop.

Pressure drop across the distributer between bottom and top portions (10 mm above and 10 mm beneath) as observed during third CFD analysis (Figure 4c) shows large variation, ranging from 11 KPa to 448 KPa as the diameter increased from 6 mm to 1 mm. As the diameter go on increasing, the pressure drop decreases, resulting in lower jet velocity and hence poor velocity distribution in the cylindrical column.

While investigating the effect of distributer angle inclination on the velocity distribution within the cylindrical container, distributers with four different configurations were considered for analysis (CFD-2). Figures 5a–c depict hole design at 13°, 15° and 17° inclinations after modelling. It is evident from the figures that percentage of opening area is more in the case of lower angles. Following observations can be made from the Figure 5 representing velocity distribution in cylinder at different heights varying distributer hole inclination (a) Maximum jet velocity of 60–70 m/s in the range of 0–200 mm is in the case of angle inclination 15° only when compared to all other configurations (b) The velocity get weakened above the first half of the cylindrical height (c) At 15° inclination the air column in the plenum chamber assumes a near cylindrical pattern (Figure 5b) (d) At 15° the swirling fluidized air attains uniform, concentrated and evenly pattern for the bottom 1/3rd portion of the cylindrical container as compared to other two hole inclinations (Figure 5b) which is similar to the last case of air-inlet velocity at 4 m/s. (Figure 3b).

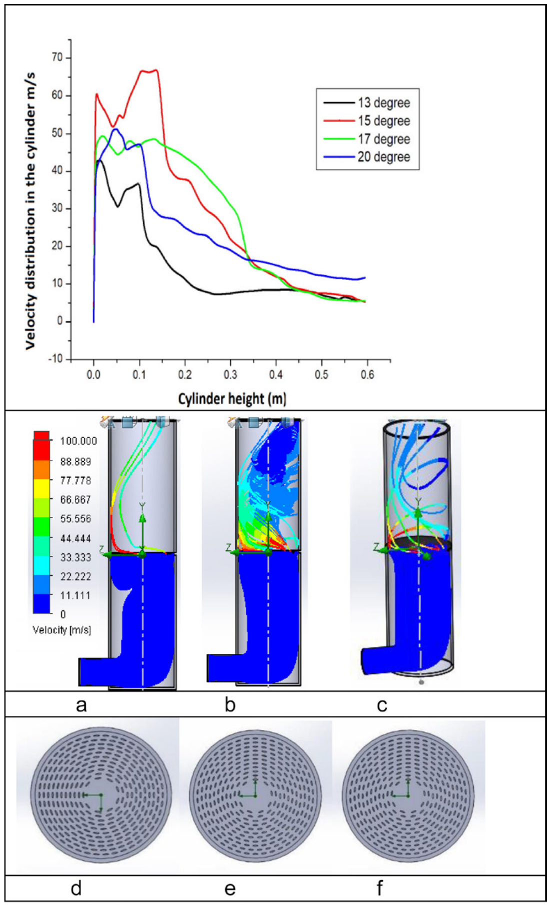

Fig 5 | Velocity distribution in cylinder at different heights varying distributer hole inclination. (a) 13°, (b) 15°, (c) 17°, (d) 13°, (e) 15°, (f) 17°

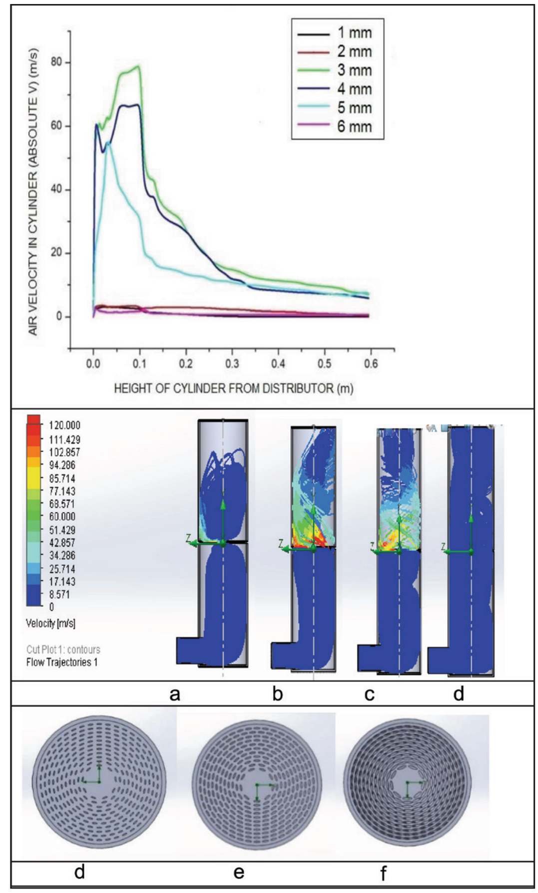

Fig 6 | Velocity distribution in cylinder at different heights varying distributer hole diameter. (a) 2 mm, (b) 3 mm, (c) 4 mm, (d) 6 mm, (d) 2 mm, (e) 3 mm, (f) 4 mm

Better uniformity in the case of 15° inclination can be explained as follows. Since the air emerging out of the inclined holes possess two components (v cos α and v sinα) as explained in Introduction part, an increase in α will weaken swirling motion and strengthen the fluidizing motion. At lower angles the swirling motion will be predominant. However at 15°, both the components generate a uniform flow with maximum velocity encompassing the bottom 1/3rd portion of the cylinder which confirms the experimental findings as reported by Paulose M. M and Sreenivasan Raghavan et al.

While investigating the effect of distributer hole diameter on the velocity distribution within the cylindrical container, distributers with six different configurations were considered for analysis (CFD-3) as per the boundary conditions applied as in Table 1. Figure 6d–f represent three different configurations with diameters 2, 3, and 4 mm respectively after modelling. The following observations are made from the Figure 6 representing velocity distribution in cylinder at different heights varying distributer hole diameter (a) the percentage area of opening increases with the diameter of the hole (Figures 6d–f). (b) Highest velocity in the range of 75–80 m/s is observed within 130 mm height as depicted in the graph in the case of diameter 3 mm. (c) Swirling fluidized flow pattern with better uniformity and concentration is observed for the bottom 1/4th portion when diameter of the hole is 3 mm (Figure 6), (d) Air jet velocity is in the range of 0–10 m/s in the second half portion of the cylinder, (e) When the hole size is too small (1 and 2 mm) and too large (6 mm) the air circulates within the container with negligible speed (f) At 3 mm dia the air column in the plenum chamber assumes a near cylindrical pattern (Figure 6b) when compared to 2 and 4 mm dia holes (Figures 6a and c). Lower value of jet velocities when large diameter holes are used can be explained in the light of pressure drop observed across the distributer planes 10 mm below and above as shown in Figure 4c. As the diameter go on increasing, the pressure drop decreases, resulting in lower jet velocity and hence poor velocity distribution in the cylindrical column. The CFD analysis results are in agreement with experimental findings by Paulose M. M as explained in the Introduction part.

The CFD-4 analysed the effect of plenum chamber depth on the velocity distribution within the cylindrical container by applying the boundary conditions as shown in the Table 1. Figure 7 represents six different plenum chamber configurations with depths 300, 400, 500, 600, and 700 mm. The following observation are made from the Figure 7 representing velocity

 DOI: https://doi.org/10.70389/PJS.100254 | Premier Journal of Science 2025;15:100254

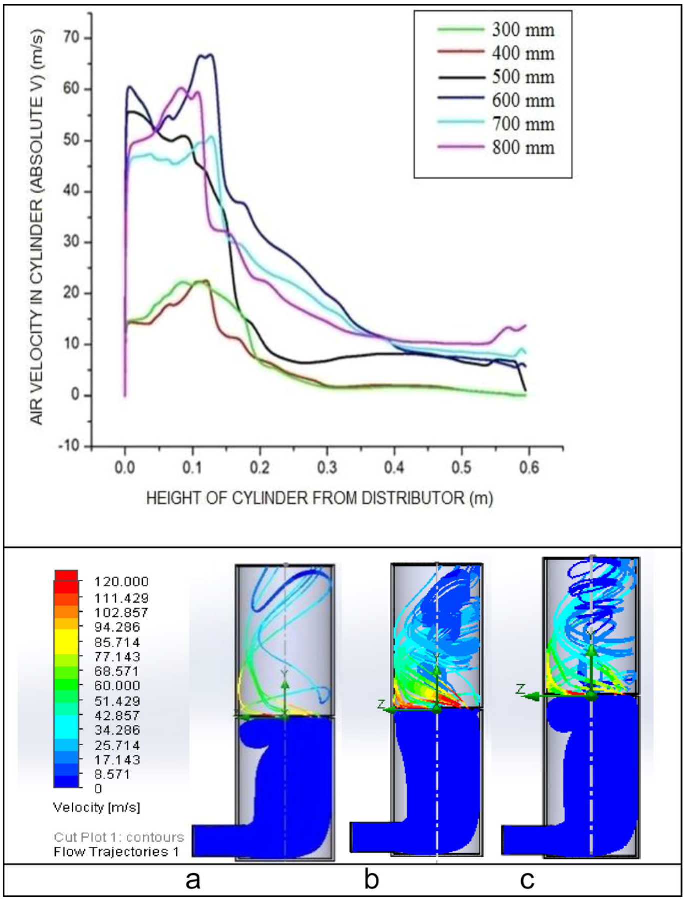

Fig 7 | Velocity distribution in cylinder at different heights varying Plenum chamber depth (a) 500 mm, (b) 600 mm, (c) 700 mm

distribution in cylinder at different heights varying the plenum chamber depth. (a) Highest velocity in the range of 60–70 m/s observed within 150 mm height as depicted in the graph in the case plenum chamber depth as 600 mm (b) In the case of low plenum chamber depths of 300 and 400 mm, the velocity curves show peak velocity of 20 m/s only (c) Velocity of the air become negligible in the top half portion of the cylinder (d) When the plenum chamber depth is 600 mm, the air flow pattern within the plenum chamber assumes the shape of a near - cylindrical column as per simulation images as in Figures 7a–c. (e) Better uniformity of air within the cylindrical column is observed in the case of plenum chamber depth 600 mm.

Table 3 | Optimized design parameters to get best velocity distribution within the cylindrical container

Hole Angle of Inclination in the Distributer	15°
Hole diameter	3 mm
Plenum chamber depth	600 mm
Velocity of air inlet to plenum chamber	4 m/s
Region of maximum velocity in the cylindrical container	50–170 mm height from the distributer level

This phenomenon can be explained as follows. Air enters the plenum chamber from bottom tangentially, and attains a uniform swirling upward pattern. For a certain optimized depth of plenum chamber, a uniform and steady swirling air column enters smoothly into the inclined hole and emerges at high jet velocity in cylindrical column (above distributor). Beyond the optimized depth of plenum chamber, the swirling pattern of air in plenum chamber weakens and the jet velocity of emerging air from the distributor hole reduces. Uniform distribution of air velocity observed within the container when the plenum chamber depth is 600 mm. On other hand, with lower depths of plenum chamber, the air column does not get enough height to assume a cylindrical pattern within the plenum chamber.

The computational fluid dynamics (CFD) analysis of the preceding sections proves that velocity distribution as well as the maximum optimized at a height ranging from 0 mm to 180 mm from the distributer plate. In order to experimentally verify the findings, a work piece of aluminium was subjected to SFBM on the experiment setup powered by a centrifugal blower (Table 3).

Conclusions

In continuation with the ongoing research regarding the feasibility of SFBM as a surface modification process, the current research focussed on the optimization of various SFB design parameters for a given set of design dimensions of distributer plate with inclined holes. In the present case a distributer with diameter-300 mm, thickness-10 mm, no. of holes-285, diameter of plenum chamber-300 mm, diameter of plenum chamber-300 mm was considered. The SFB design parameters subjected to CFD analysis were plenum chamber depth, velocity of air inlet, inclination and diameter of distributer holes. The aim of the CFD analysis was to identify the best work piece positioning with maximum value of air jet velocity within the cylindrical container which will result in better metal removal and surface finish. Following conclusions are drawn from the investigations.

1. Uniform and even velocity distribution with maximum value (65–75 m/s) was observed when the distributer inclination is 15°, hole diameter is 3 mm, plenum chamber depth is 600 mm and inlet velocity is 4 m/s. These values can be taken as optimized design parameters
2. The swirling fluidizing activity gets weakened above 200 mm height due to the weakening of the three velocity components
3. CFD analysis underlines that better velocity distribution and maximum velocity is observed within 1/3rd (0–200 mm) height of the cylindrical container
4. CFD analysis results were further validated experimentally on aluminium specimen while subjected to SFBM. The results demonstrate that region encompassing 40–115 mm can result in better surface modification during SFBM

5. Influence of pressure drop across the distributer on the jet velocity was investigated for different design parameters during CFD analysis.

References

1 Barletta M. A new technology in surface finishing—Fluidized Bed Machining (FBM) of aluminum alloys. Int J Mater Process Technol. 2006;173(2):157–65. https://doi.org/10.1016/j.jmatprotec.2005.11.020

2 Sreenivasan B, Jones CA. Helicity generation and subcritical behaviour in rapidly rotating dynamos. J Fluid Mech. 2011;688:5–30. https://doi.org/10.1017/jfm.2011.233

3 Srinivasan B, Raghavan, Vijay R. Hydrodynamics of a swirling fluidized bed. Chem Eng Process Process Intensif. 2002;41(2):99–106.

4 Jun GJ, Raghavan VR, Sing CY. Experimental study on the hydrodynamics of a swirling fluidised bed. Appl Mech Mater. 2012;229–231:756–60. https://doi.org/10.4028/www.scientific.net/AMM.229-231.756

5 Paulose MM, Narayanan N. Hydrodynamic study of swirling fluidized bed and the role of distributor. Thesis submitted to the Cochin University of Science and Technology, in partial fulfilment of the requirements for the award of the degree of Doctor of philosophy; 2006. Available from: https://dyuthi.cusat.ac.in/xmlui/handle/purl/911

6 Barletta M. Progress in abrasive fluidized bed machining. J Mater Process Technol. 2009;209(20):6087–102. https://doi.org/10.1016/j.jmatprotec.2009.04.009

7 Faizal M, Seri SM, Al-Hafiz M, Raghavan VR. CFD studies on velocity distribution of air in a swirling fluidized bed. Adv Mater Res. 2012;468–471:25–9. https://doi.org/10.4028/www.scientific.net/AMR.468-471.25

8 Francis NK, Viswanadhan KG, Poulose MM. Swirling abrasive fluidized bed machining: effect of process parameters on machining performance. Int J Mater Manuf Process. 2015;30(2):852–7. https://doi.org/10.1080/10426914.2014.973580

9 Francis NK, Viswanadhan KG, Poulose MM. SAFBM of softer materials: an investigation into micro-cutting mechanisms and the evolution of surface roughness profile. Int J Mater Manuf Process. 2015;31(7):969–75. https://doi.org/10.1080/10426914.2015.1090585

10 Zhang Y, Zhu J, Lyu Q, Liu J, Pan F, Zhang J. The ultra-low NOx emission characteristics of pulverized coal combustion after high temperature preheating. Fuel. 2020;277:118050. https://doi.org/10.1016/j.fuel.2020.118050

11 Simanjuntak ME, Sitorus MBH, Kamil I, Br Ginting B, Sutrisno T, Widodo WA, et al. Kinetic analysis and mathematical modeling of low-rank coal drying by using swirl fluidized bed dryer on varied angles of guide vane and temperatures. Energy Sources A Recovery Util Environ Eff. 2024;46:3263–77. https://doi.org/10.1080/15567036.2024.2317435

12 Zhang S, Li H, Deng Z, Chen Y, Guo P, Yang Q, et al. Effect of the combination of squid-fin-inspired wall and internal vortex generator on methane reduction in a micro-fluidized bed reactor. Fuel. 2025;381:133476. https://doi.org/10.1016/j.fuel.2024.133476

13 Sitorus A, Novrinaldi, Putra SA, Cebro IS, Bulan R. Modelling drying kinetics of paddy in swirling fluidized bed dryer. Case Stud Thermal Eng. 2021;28:101572. https://doi.org/10.1016/j.csite.2021.101572

14 Ban Y, Liu L, Du J, Ma C. Investigation of the treatment efficiency and mechanism of microporous flocculation magnetic fluidized bed (MFMFB) reactor for Pb(II)-containing wastewater. Sep Purif Technol. 2024;334:125963. https://doi.org/10.1016/j.seppur.2023.125963

15 Pietrobono F, Rubino G, Tagliaferri V, Trovalusci F. Sample position inside abrasive fluidized bed to obtain morphology uniformity. Int J Adv Manuf Technol. 2019;103(1–4):49–61. https://doi.org/10.1007/s00170-019-03539-y

16 Atzeni E, Barletta M, Calignano F, Iuliano L, Rubino G, Tagliaferri V. Abrasive fluidized bed (AFB) finishing of AlSi10Mg substrates manufactured by direct laser sintering (DMLS). Addit Manuf. 2016;10:15–23. https://doi.org/10.1016/j.addma.2016.01.005

17 Quadrini F, Tagliaferri V, Polini R. Effect of coating roughness on performance of small CVD diamond coated tools. Mach Sci Technol. 2008;12:390–404. https://doi.org/10.1080/10910340802292084

18 Ravi Sankar M, Jain VK, Ramkumar J. Effect of abrasive medium ingredients on finishing of Al alloy and Al alloy/SiC metal matrix composites using rotational abrasive flow finishing. Appl Mech Mater. 2012;110–116:1328–35. https://doi.org/10.4028/www.scientific.net/AMM.110-116.1328

19 Kim T, Lee H. Simulation and experimental analysis of abrasive fluidized bed machining process. J Mech Sci Technol. 2020;34(5):2153–60. https://doi.org/10.1007/s12206-020-0436-5